

Dynamical modeling of the Deep Impact dust ejecta cloud

Tanyu Bonev¹ *, Nancy Ageorges², Stefano Bagnulo², Luis Barrera³, Hermann Bönnhardt⁴, Olivier Hainaut², Emmanuel Jehin², Hans-Ullrich Käuff², Florian Kerber², Gaspare LoCurto², Jean Manfroid⁵, Olivier Marco², Eric Pantin⁶, Emanuela Pompei², Ivo Saviane², Fernando Selman², Chris Sterken⁷, Heike Rauer⁸, Gian Paolo Tozzi⁹, and Michael Weiler⁸

¹ Institute of Astronomy, Bulgarian Academy of Sciences, Sofia, Bulgaria
tbonev@astro.bas.bg

² European Southern Observatory

³ Universidad Metropolitana de Ciencias de la Educacion, Santiago de Chile, Chile

⁴ Max-Planck-Institut für Sonnensystemforschung, Katlenburg-Lindau, Germany

⁵ Université de Liège, Belgium

⁶ Commissariat Energie Atomique, F-91191 Gif-sur-Yvette, France

⁷ Vrije Universiteit Brussel, Belgium

⁸ Deutsches Zentrum für Luft und Raumfahrt, Germany

⁹ Istituto Nazionale di Astrofisica (INAF) Osservatorio di Arcetri, Italy

Summary. The collision of Deep Impact with comet 9P/Tempel 1 generated a bright cloud of dust which dissipated during several days after the impact. The brightness variations of this cloud and the changes of its position and shape are governed by the physical properties of the dust grains. We use a Monte Carlo model to describe the evolution of the post-impact dust plume. The results of our dynamical simulations are compared to the data obtained with FORS2¹ to derive the particle size distribution and the total amount of material contained in the dust ejecta cloud.

1 Introduction

Dynamical modeling of the dust coma is often used to constrain properties of the dust grains released from a cometary nucleus. An excellent summary of these efforts is given by [9]. In his review M. Fulle mentions that, in order to reach a better fit between model and observation, modelers are often pressed to make the assumption of time-independent particle size distribution (PSD). Observations of the Deep Impact (DI) dust ejecta cloud represent a special case in this respect. The time of the impact is exactly known (UT 5:52 on July 4, 2005) and the time interval in which particles excavated by the impact leave

* TB is indebted to the organizers for supporting his participation at the conference "Deep Impact as a World Observatory Event - Synergies in Space, Time, and Wavelength".

¹ FORS stands for FOcal Reducer and low dispersion Spectrograph for the Very Large Telescope (VLT) of the European Southern Observatory (ESO).

the circumnuclear region is relatively short (with some exceptions which are discussed below). Thus, time-dependence of the PSD could be excluded to the first approximation in model calculations (valid only if no further processing of the particles takes place later). The DI ejecta cloud was observed from the DI spacecraft [1] and from a great number of ground based observatories [11]. We present observations of comet 9P/Tempel 1 (hereafter 9P) obtained with FORS2 at the VLT of ESO in Paranal. We use a Monte Carlo model to describe the DI ejecta cloud observed during the 4 days after the impact. Inversion of our model allows to derive the PSD and, under appropriate assumptions, to make an estimation of the total mass of dust released by the impact and ejected with velocities higher than the escape velocity of 9P.

2 The Observations

The images used in this analysis were obtained with FORS2² [3]), mounted at the VLT Antu. To secure a basis for comparison with the post-impact data several images were taken about 6 hours pre-impact, shortly before the time when the comet set at Paranal. During the next 4 nights images were obtained at 17.8, 42.4, 66.3, 89.4 hours after the impact. The heliocentric distance of 9P was 1.51 AU, almost constant during the observing period, as the comet was at perihelion on July 5.35. The geocentric distance increased from 0.89 to 0.91 AU, and the pixel scale changed correspondingly from 162 km/px to 167 km/px. The images were calibrated to fluxes and then transformed to Af, the Albedo-filling factor product [2]. Figure 1 shows the R-band post-impact images with subtracted contribution of the pre-impact coma. These images are used in the further analysis.

The quantity Af is convenient for comparison with theoretical models as it is directly related to the total cross-section of the scattering dust particles at any particular picture element. The total scattering cross-section \times Albedo ($A \times S$) of all dust particles produced by the impact was obtained by integration over the whole area covered by the post-impact clouds shown in figure 1. The derived values are presented in table 1. Note the reduction of $A \times S$ with time.

Table 1. Values of the product Albedo \times total scattering cross-section ($A \times S$) derived from the post-impact images with subtracted pre-impact coma

Time after impact, hour	$A \times S$ km ²
17.8	7.6
42.4	5.8
66.3	5.1
89.4	3.2

² for details see <http://www.eso.org/instruments/fors1/>

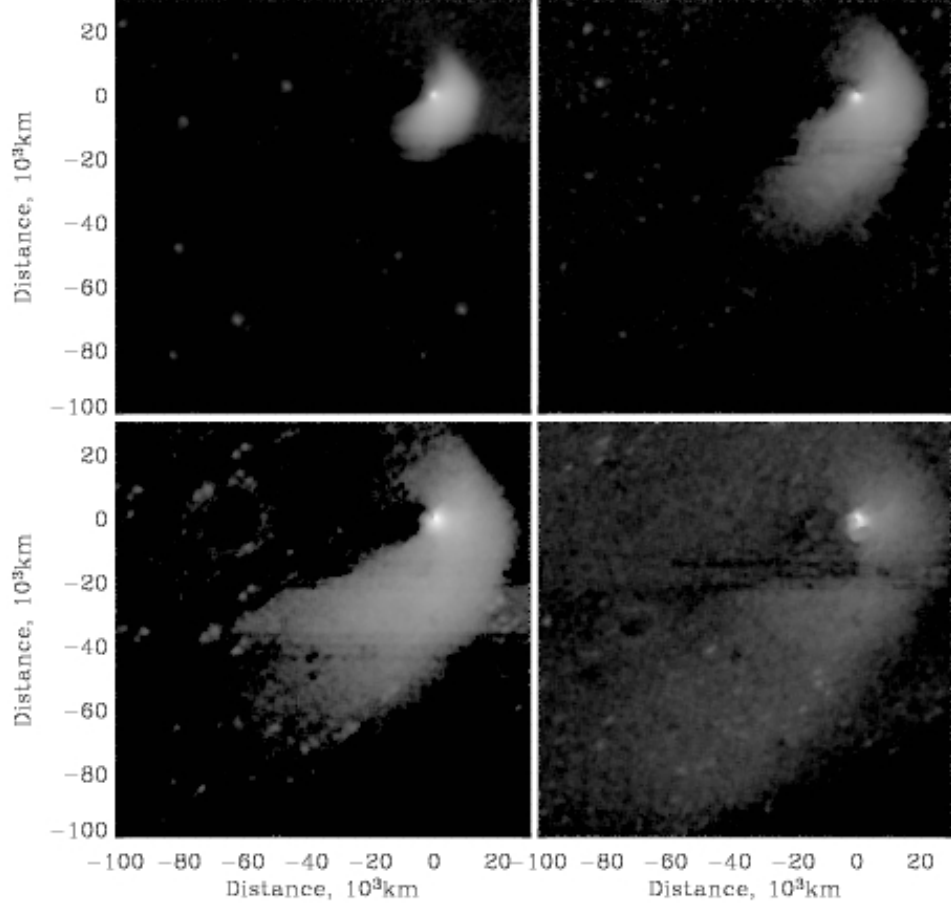


Fig. 1. Sequence of R-band images representing the dust cloud induced by the impact. From the left upper to the right lower corner the four panels show the changing dust distribution during the four post-impact days. Each panel contains the difference of the particular R-band image with a pre-impact image. North is up, East to the left. The projected direction to the Sun is at 291 degree, counted from North to East

3 The model

3.1 Initial conditions

In the numerical model described below we use particles of radii from 0.25 to 250 μm . To run the model an initial guess for the velocity dependence on particle size is needed. The shape of the ejecta cloud (figure 1) shows that after the impact the dust expansion is initially at position angle (P.A.) 240° (the projected direction to the Sun is at P.A. 291°). Later it is deflected by the

solar radiation pressure in antisolar direction. Four days after the impact most of the dust is spread over a large area in antisolar direction. But even on the fourth day (90 hour after the impact) dust particles are still found in direction to the Sun. We suppose that these are larger particles which are ejected with lower velocities and which are less influenced by the radiation pressure in comparison to smaller particles. Assuming that the well expressed boundary in direction to the Sun is the stagnation region of particles ejected with velocity v , and measuring the distance d from the comet to this boundary, we can write $v = bt$ and $v^2 = 2bd$, where b is the radiation pressure acceleration. Measured values of d , and derived values for the velocity and acceleration are given in table 2. The acceleration is used to derive values for β , the ratio of gravitational force to the force of radiation pressure. Finally, from β , we derive the radii of the particles, a , using the dependence [5]: $\beta = 0.585 \times 10^{-4} Q_{pr}/(\rho a)$, where ρ is the density of the particles. The rough estimation of the particles' radii, listed in table 2, was made with an assumed value for the radiation pressure efficiency, $Q_{pr} = 1.7$, with a density, $\rho = 1 \text{ g cm}^{-3}$. Our

Table 2. Apex distance, measured in the four images, and derived values for the velocity, acceleration, and particle size

UT Day of July 2005	Time after impact hour	Distance 10 ³ km	Terminal velocity km/s	Acceleration km/s ²	β values	Particle radius μm
4.972	17.8	16.5 +/- 2	0.51 +/- 0.06	8.03e-6	3.01	0.3
5.995	42.4	21.0 +/- 3	0.28 +/- 0.04	1.81e-6	0.68	1.5
6.993	66.3	25.0 +/- 4	0.21 +/- 0.03	8.77e-7	0.33	3.0
7.955	89.4	29.0 +/- 5	0.18 +/- 0.03	5.60e-7	0.21	4.8

approach yields the initial velocities of the particles. Therefore the values in table 2 are about 2 times larger compared to the mean velocities given by many other observers ([11], [12]). The derived velocity-size dependence follows a power law with power index close to -0.4. This dependence resembles the velocities obtained from theoretical models of the natural gas-dust interaction in the vicinity of a cometary nucleus ([7], [6]), as well as the velocities derived from models describing the dust coma and tail ([9] and references therein). Initial guess for the location of the impact was found by the constraints coming from (a) the observed projected expansion direction of the ejected cloud, (b) the rotation axis orientation ([4]), and (c) the latitude of the impact (M. A'Hearn, private communication).

3.2 Direct Monte Carlo calculations

The velocity law and the impact location were determined more precisely in a process of trial and error. We calculated a series of models with values around

the initial guess until we reached a satisfying morphological reproduction of the observed dust distribution for the four observations.

In the model used for description of the impact cloud we use 1 million dust particles which are emitted for a period of 20 minutes starting at the moment of the impact. These particles are distributed in 100 emission events along 200 emission directions randomly spaced in a cone with full opening angle of 180 degree. The particles are assumed compact with density of 1 g/cm³ and radii distributed logarithmically in 51 bins, in the range from 0.25 to 250 micrometer. After ejection the particles move along Keplerian orbits under the influence of gravity and radiation pressure. Their positions are calculated for the times of observation, the contributions of the different sizes are weighted with an initial guess for the PSD and integrated along the line of sight. The modeled brightness, at position (x,y) is described by:

$$B(x, y) = \sum_{i=0}^{50} K_i \times S_i(x, y) \quad (1)$$

where $S_i(x,y)$ is the scattering area produced by the particles of one particular size, i , and K_i are the coefficients to be found.

3.3 Inversion of the model

The coefficients K_i in equation 1 are derived by comparing the modeled brightness $B(x, y)$ to the observed one and by minimizing the differences through linear regression. Figure 2 shows the result of the fit to the dust cloud observed 17.8 hours after the impact. The full line in the left panel represents the initial guess for the PSD, a power law with power index -3.0. Triangles show the solution of equation 1 converted to the number of particles of given size. Particles larger than about 20 micron scatter strongly around the mean distribution. These large grains are expelled with lower velocities and their motion is less influenced by the radiation pressure in comparison to the smaller particles. Therefore large particles of several size bins coexist in a relatively small region around the nucleus and compete in the process of linear regression. It seems that we should simply restrict the upper limit of particle radii to smaller values. Indeed, this makes the solution more stable, but at the same time it removes the contribution to the brightness close to the nucleus. In order to reproduce the enhanced brightness of the ejecta plume observed in this region, particles of radii as high as 250 μm are needed. Extrapolation of our initial velocity law shows that these large particles have velocities still above the escape velocity of 9P, 1.7 m/s [1]. The right panel in figure 2 shows the cumulative mass distribution of the dust. We derive a total mass of the dust in the ejecta cloud of 3.7 kiloton.

The inversion of the model succeeded only in the case of the ejecta cloud observed 17.8 hours after the impact, which is characterized by the highest signal-to-noise ratio. The dust distribution in the next images was reproduced

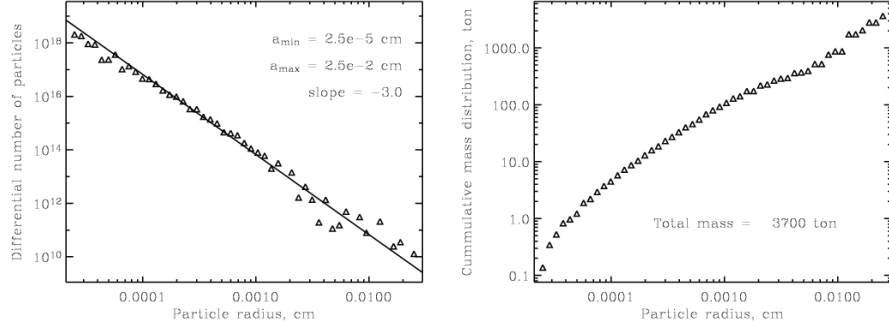


Fig. 2. The differential particle size distribution (left) and the cumulative mass distribution (right) derived from the fit of the model to the observations

with the parameters found from the fit to the first post-impact observation. The four modeled ejecta clouds corresponding to the four observations are presented in figure 3.

4 Results and discussion

The PSD derived from the fit to the ejecta cloud observed 17.8 hours after the impact follows a power law with mean power index -3.0. In the detailed model developed by [8] particles of radii $< 20 \mu\text{m}$ are used and a slope of the differential dust size distribution -3.2 is found. Light curves of the impact plume were obtained from space ([10] and from the ground (Pittichova et al. (presentation at ACM'2005))). These light curves show similar behavior, first a sharp increase in a time interval dependent on the aperture used, and second, a gradual decrease of the brightness. The decreasing wing of these lightcurves is well described by subtracting the contribution of small particles leaving the detector diaphragm with the velocities used in our model and distributed in accordance with a PSD with slope -3.0.

The velocity distribution of the impact ejecta is similar to velocity laws which describe the natural activity of a comet. We came to this conclusion empirically, without analyzing possible mechanisms of particle acceleration related to the impact itself. Our conclusion is based on the particles having velocities greater than the escape velocity of 9P. At the same time our images with removed pre-impact coma show a brightness around the nucleus of the comet. Schleicher et al. [12] point to the same feature in their morphological analysis of the ejecta plume. They explain the enhanced brightness close to the nucleus with the existence of large, heavy particles that have been ejected with velocities below the escape velocity of the comet. A future combined analysis of the motion of particles ejected with velocities above and below the escape limit could be of interest for understanding the acceleration mechanism of particles produced by the impact.

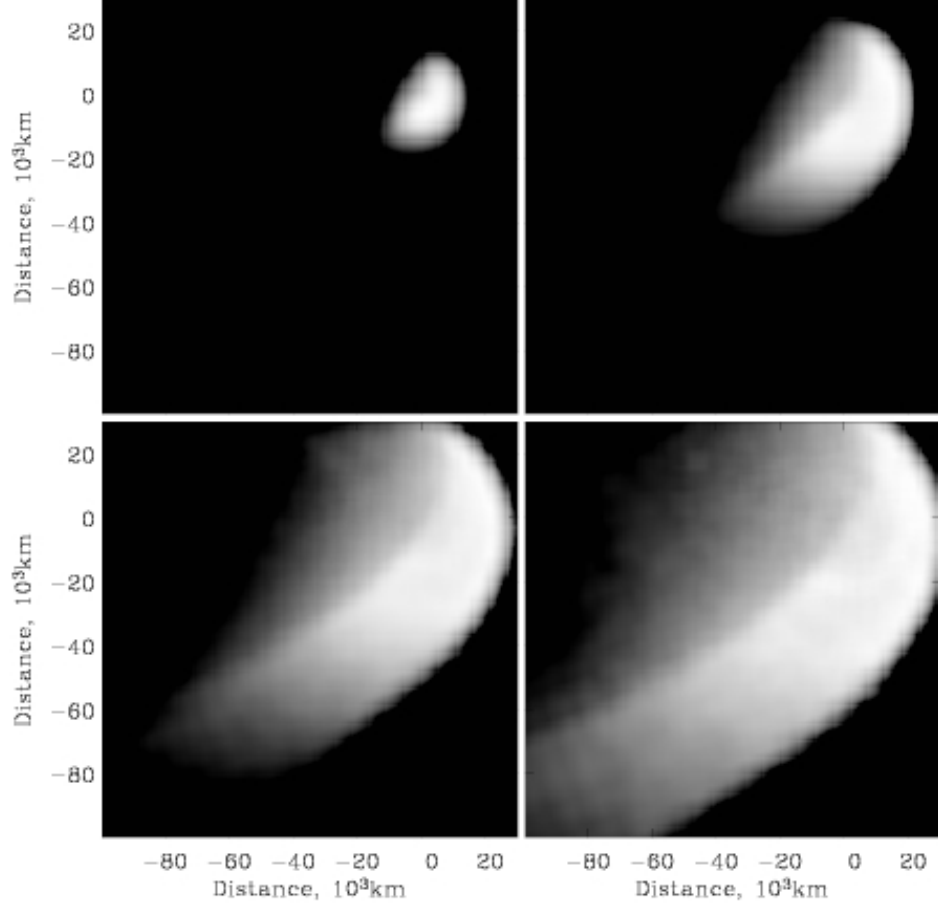


Fig. 3. Models of the DI dust ejecta cloud corresponding to the four observations

In section 2 we have shown that the product scattering area \times Albedo decreases with increasing time from the impact. It is interesting to extrapolate this trend back in time and to make a comparison with data obtained during the first hours after the impact. The Rosetta team registered a peak of the light curve 1 hour after the impact [10]. From the difference between this value and the pre-impact level these authors derived a total $A \times S$ of the newly created dust particles of 33 km^2 . This is much greater compared to the value expected from the back extrapolation of our measurements, even if we fit them with an exponential law. This is an indication that the decrease of $A \times S$ should have been faster during the first hours after the impact. Possible explanation could be the fragmentation of particles with sizes comparable to the wavelength of observations. Their smaller products will scatter effectively at shorter wavelengths and, under given conditions, could become invisible

in the R-band. Although this mechanism appears possible further work is needed to support it with quantitative arguments.

5 Conclusions

We used a dynamical model to describe the dust ejecta created by Deep Impact. The applied velocity-size dependence was derived empirically. Particle with radii in the range 0.25 - 250 μm were considered. We found a best fit to the dust cloud 17.8 hours after the impact with differential particle size distribution following a power law with index -3.0. The total mass of the dust dust ejecta having velocities greater than the escape velocity is 3700 ton.

References

1. M. A'Hearn, M. Belton, W. Delamere et al: Science, **310**, 258 (2005)
2. M. A'Hearn, D. Schleicher, R. Millis et al: Astronomical Journal, **89**, 579 (1984)
3. I. Appenzeller, K. Fricke, W. Furtig et al: The Messenger, **94**, 1 (1998)
4. M. Belton, P. Thomas, B. Carcich et al: The Spin State of 9P/Tempel 1. In *Proceedings 37th Annual Lunar and Planetary Science Conference, 2006*, ed by S. Mackwell, E. Stansbery, 1487
5. J. Burns, P. Lamy, S. Soter: Icarus, **40**, 1 (1979)
6. J.-F. Crifo: Hydrodynamic models of the collisional coma. In *ASSL Vol. 167: IAU Colloq. 116: Comets in the post-Halley era, 1991*, ed by R. Newburn, M. Neugebauer, J. Rahe, pp 937–989
7. T. Gombosi: A heuristic model of the Comet Halley dust size distribution, In *ESA SP-250: ESLAB Symposium on the Exploration of Halley's Comet. Volume 2: Dust and Nucleus, 1986*, ed by B. Battrick, E. Rolfe, R. Reinhard, pp 167–171
8. L. Jorda, P. Lamy, G. Faury et al: Icarus, **187**, 208 (2007)
9. M. Fulle: Motion of cometary dust, in *Comets II*, ed by M. Festou, H.U. Keller, H.A. Weaver, 565 (2004)
10. M. Küppers, I. Bertini, S. Fornasier et al: Nature, **437**, 987 (2005)
11. K. Meech, N. Ageorges, M. A'Hearn et al: Science, **437**, 265 (2005)
12. D. Schleicher, K. Barnes, N. Baugh: Astronomical Journal, **131**, 1130 (2006)